4. ANKARA INTERNATIONAL AEROSPACE CONFERENCE **AIAC-2007-011**
10-12 September, 2007 - METU, Ankara

RESPONSE SURFACE METHOD FOR THE MAXIMIZATION OF THRUST IN FLAPPING AIRFOILS

Mustafa Kaya* and Ismail H. Tuncer†
Middle East Technical University
Ankara, Turkey

ABSTRACT

The flapping parameters of an airfoil which undergoes a combined non-sinusoidal pitching and plunging motion are optimized for maximum thrust. The non-sinusoidal, periodic flapping motion is described using Non-Uniform Rational B-Splines (NURBS). The Response Surface Methodology (RSM) is employed for the optimization of NURBS parameters in a parallel computing environment. Unsteady, laminar flows are computed by a Navier-Stokes solver in parallel. It is shown that the parallel optimization process with RSM for 3 optimization variables is about one order of magnitude more efficient and faster than the gradient based optimization process.

INTRODUCTION

Based on observations on flying birds, insects, and swimming fish, it appears that flapping wings may be favorable for flights of very small scale vehicles, so-called micro-air vehicles (MAVs) with wing spans of $15\ cm$ or less. The current interest in the research and development community is to find the most energy efficient airfoil adaptation and flapping wing motion technologies capable of providing the required aerodynamic performance for a MAV flight.

The recent experimental and computational studies investigated the kinematics, dynamics and flow characteristics of flapping wings, and shed some light on the lift, drag and propulsive power considerations[12, 16]. In their experimental study, Lai and Platzer[17] investigate drag-producing wake flows and thrust-producing jet-like flows downstream of a plunging airfoil. Water tunnel flow visualization experiments by Jones et al.[18] provide a considerable amount of information on the wake characteristics of flapping airfoils. Another water tunnel study is conducted by Heatcote et al.[3] to observe the effect of spanwise flexibility on the thrust, lift and propulsive efficiency of a rectangular wing in a pure plunge motion. They find that introducing a degree of spanwise flexibility is beneficial in terms of high thrust and propulsive efficiency. In their experiments, Anderson et al.[19] observe that the phase shift between pitch and plunge oscillations plays a significant role in maximizing the propulsive efficiency. A recent experimental study by Schouveiler et al.[6] show that high thrust and efficiency conditions can be achieved together for some range of flapping parameters.

Hover et al.[7] use sinusoidal and non-sinusoidal effective angle of attack variations in time to investigate the propulsive performance of an airfoil undergoing combined plunge and pitch motions. Lee et al.[2] identify the key physical flow phenomenon dictating the thrust generation of a plunging and/or pitching airfoil in terms of flow and/or geometry parameters.

Navier-Stokes computations performed by Tuncer and Platzer[13] show that an airfoil undergoing combined pitch and plunge oscillations, may produce high thrust at a high propulsive efficiency under certain kinematic conditions. Tuncer et al.[22, 21] also observe that the thrust and the propulsive efficiency values may be significantly increased in the case of flapping/stationary airfoil combinations in tandem. Using a Navier-Stokes solver, Isogai et al.[15] explore the effect of dynamic stall phenomena on the thrust generation and the propulsive efficiency of flapping airfoils. Young and Lai[8] show that the vortical wake structures, and the lift and thrust characteristics of a plunging airfoil are strongly dependent on the oscillation frequency and amplitude.

*GRA in Aerospace Engineering Department, Email: mkaya@ae.metu.edu.tr
†Prof. in Aerospace Engineering Department, Email: tuncer@ae.metu.edu.tr

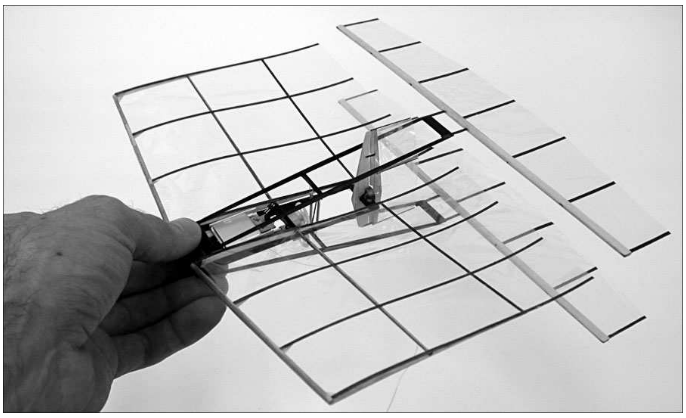

Figure 1: Flapping-wing MAV model(Jones and Platzer)

Jones and Platzer[9] recently demonstrated a radio-controlled micro air vehicle propelled by flapping wings in a biplane configuration (Figure 1). The experimental and numerical studies by Jones et al.[9, 10, 11] and Platzer and Jones[14] on flapping-wing propellers points at the gap between numerical flow solutions and the actual flight conditions over flapping wings.

In earlier studies[22, 13], the average thrust coefficient of a NACA0012 airfoil flapping sinusoidally in combined plunge and pitch is obtained for a range of reduced frequencies and amplitudes of the flapping motion. The computational and experimental findings show that the thrust generation and the propulsive efficiency of flapping airfoils are closely related to the flapping motion and flow parameters. In a later study[4], the present authors employed a gradient based optimization of sinusoidal flapping motion parameters, such as the flapping frequency, the amplitude of pitch and plunge motions and the phase shift between them, in order to maximize the thrust and/or the propulsive efficiency of flapping airfoils. It should be noted that in the sinusoidal motion, the pitch and plunge positions are based on the projection of a vector rotating on a unit circle, and the maximum plunge and pitch velocities occur at the mean plunge and pitch positions. In the following two studies[5, 1], the sinusoidal periodic motion is relaxed by replacing the unit circle with another closed curve. In the first study, an ellipse is used to define the non-sinusoidal flapping path whereas a more general closed curve based on a 3^{rd} degree Non-Uniform Rational B-Splines (NURBS) is used in the second one. The optimization of the parameters defining the ellipse and the NURBS shows that the thrust generation of flapping airfoils may further be increased on a non-sinusoidal path. In the present study, the periodic flapping motion (Figure 2) is defined using NURBS.

Response surface methodology (RSM) is mainly employed to construct global approximations to a function based on its values computed at various points[23]. The method is very useful and strong when optimization of a function is expensive and difficult in terms of computational resources. In the past, RSM approximations were commonly utilized by researches for optimization problems[23, 25, 24, 26].

In the present study, the thrust generation of a non-sinusoidally flapping airfoil is approximated using RSM. The constructed approximations are based on laminar flow solutions computed with various NURBS based non-sinusoidal flapping cases. Once the response surface approximations are constructed, maxima of the response surfaces are determined to obtain optimum flapping motions. Finally, RSM is compared to the steepest ascent method in terms of the optimization performance and the accuracy.

RESPONSE SURFACE METHODOLOGY

The main idea lying behind RSM is to build the approximate models for unknown functional relationships between some input and an output.

The average thrust coefficient, C_t, is a function of flapping parameters for fixed flight conditions. It is based on the integration of the drag coefficient over a flapping period:

$$C_t = -\frac{1}{T}\int_t^{t+T} C_d \, dt \tag{1}$$

where T is the period of the flapping motion. We can write:

$$C_t = \eta(V_1, V_2, V_3, \ldots) \tag{2}$$

where V_i's are the flapping parameters. However, the function $\eta(\vec{V})$ is unknown since it depends on the solution of the Navier-Stokes equations. Therefore, an approximation for the functional relationship, $\eta(\vec{V}) \cong g(\vec{V})$ may be constructed over some $\vec{V}$ region [23].

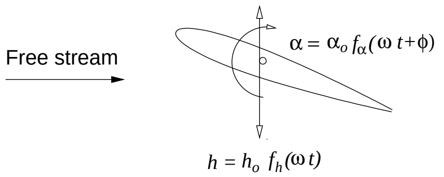

Figure 2: Flapping motion of an airfoil

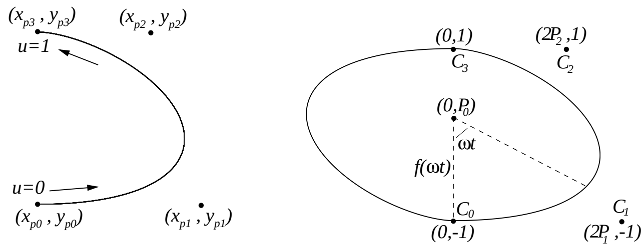

Figure 3: Flapping path defined by a 3^{rd} degree NURBS

In this study, $g(\vec{V})$, is chosen to be a quadratic function of V_i's:

$$g(V_i) = a_{11}V_1^2 + 2a_{12}V_1V_2 + 2a_{13}V_1V_3 + \ldots + a_{22}V_2^2 + \ldots \tag{3}$$

The constants, a_{ij}, in Eqn. 3 are selected to minimize the following expression:

$$\sum_{n=1}^{N} \left(g(V_i)_n - C_{tn}\right)^2 \tag{4}$$

where N is the total number of unsteady Navier-Stokes solutions (design runs) computed for several V_i combinations. The minimum value attenuated in Equation 4 is called the least-square residual.

NON-SINUSOIDAL PERIODIC PATH BASED ON NURBS

A smooth curve S based on a general n^{th} degree rational Bezier segment is defined as follows[20]:

$$S(u) = (x(u), y(u)) = \frac{\sum_{i=0}^{n} W_i B_{i,n}(u) C_i}{\sum_{i=0}^{n} W_i B_{i,n}(u)} \qquad 0 \le u \le 1 \tag{5}$$

where $B_{i,n}(u) \equiv \frac{n!}{i!(n-i)!} u^i (1-u)^{n-i}$ are the classical n^{th} degree Bernstein polynomials, and $C_i = (x_{pi}, y_{pi})$, are called control points with weights, W_i. Note that $S(u=0) = C_o$ and $S(u=1) = C_n$. A closed curve which describes the upstroke and the downstroke of a flapping path is then defined by employing a NURBS composed of two 3^{rd} degree rational Bezier segments. The control points and their corresponding weights are chosen such that the non-sinusoidal periodic function (y coordinates of the closed curve) is between -1 and 1. The periodic flapping motion is finally defined by 3 parameters. The first parameter P_o defines the center of the rotation vector on the closed curve. The remaining two parameters, P_1 and P_2 are used to define the x coordinates of the control points, which are $C_1 = (2P_1, -1)$ and $C_2 = (2P_2, 1)$ (Figure 3). The parameters P_1 and P_2 define the flatness of the closed NURBS curve.

The x and y coordinates on the periodic NURBS curve may be obtained as a function of the parameter u:

$$x(u) = \frac{2P_1 u(1-u)^2 + 2P_2 u^2(1-u)}{(1-u)^3 + u(1-u)^2 + u^2(1-u) + u^3} \qquad y(u) = \frac{-(1-u)^3 - u(1-u)^2 + u^2(1-u) + u^3}{(1-u)^3 + u(1-u)^2 + u^2(1-u) + u^3} \tag{6}$$

The non-sinusoidal periodic function, f, is then defined as:

$$f\left(u(\omega t)\right) = y(u) \equiv f(\omega t) \tag{7}$$

where

$$\tan(\omega t) = -\frac{x(u)}{y(u) - P_o} \tag{8}$$

For a given ωt position, Equation 8 is solved for u. Once u is determined, $y(u) \equiv f(\omega t)$ is evaluated using Equation 6.

NUMERICAL SOLUTION METHOD

2-D unsteady viscous flows around a flapping airfoil are computed by solving the Navier-Stokes equations on a moving C-grid. The grid is partitioned into overlapping subgrids, and computations on subgrids are performed in parallel (Figure 4). A gradient based optimization is employed for the optimization of flapping motion parameters to maximize the average thrust coefficient and/or the propulsive efficiency.

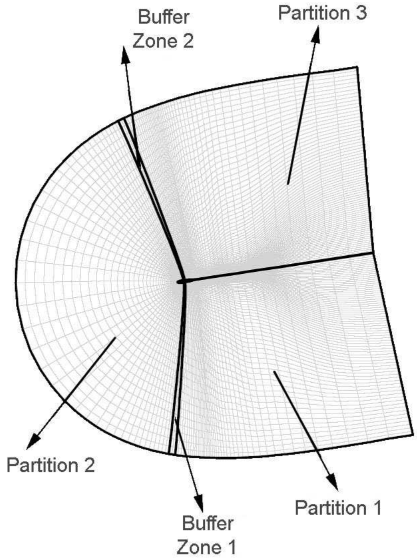

Figure 4: Domain decomposition with 3 partitions

Navier-Stokes Solver

The strong conservation-law form of the 2-D, thin-layer, Reynolds averaged Navier-Stokes equations is solved on each subgrid. The governing equations in a curvilinear coordinate system, (ξ, ζ), are given as

$$\partial_t \hat{\mathbf{Q}} + \partial_\xi \hat{\mathbf{F}} + \partial_\zeta \hat{\mathbf{G}} = Re^{-1} \partial_\zeta \hat{\mathbf{S}} \tag{9}$$

where $\hat{\mathbf{Q}}$ is the vector of conservative variables, $\hat{\mathbf{F}}$ and $\hat{\mathbf{G}}$ are the convective flux vectors, and $\hat{\mathbf{S}}$ is the thin layer approximation of the viscous fluxes in the ζ direction normal to the airfoil surface. The convective fluxes are evaluated using the third order accurate Osher's upwind biased flux difference splitting scheme. The discretized equations are solved by an approximately factored, implicit algorithm[22, 13].

Boundary Conditions

The flapping motion of the airfoil is imposed by moving the airfoil and the C-grid around it. The combined plunge, h, and pitch, α, motions of the airfoil are described by

$$h = -h_0\, f_h(\omega t), \qquad \alpha = -\alpha_0\, f_\alpha(\omega t + \phi) \tag{10}$$

where h_0 and α_0 are the plunge and pitch amplitudes, f is the periodic function based on NURBS, ω is the angular frequency which is given in terms of the reduced frequency, $k = \frac{\omega c}{U_\infty}$. ϕ is the phase shift between the plunging and the pitching motions. The pitch axis is located at the mid-chord.

At the overlapping boundaries of the subgrids, at every time step, the conservative flow variables are exchanged among the subgrids.

Optimization based on the Steepest Ascent Method

The objective function, O, is the average thrust coefficient, C_t, over a flapping period. The gradient based optimization process is based on following the steepest ascent direction of the objective function, O. The direction of the steepest ascent is given by the gradient vector of the objective function:

$$\vec{\nabla} O(\vec{V}) = \frac{\partial O}{\partial V_1}\vec{v_1} + \frac{\partial O}{\partial V_2}\vec{v_2} + \cdots$$

where V_i's are the optimization variables, and the $\vec{v_i}$'s are the corresponding unit vectors in the variable space.

The components of the gradient vector are then evaluated numerically by computing the objective function for a perturbation of all the optimization variables one at a time. It should be noted that the evaluation of these vector components requires an unsteady flow solution over a few periods of the flapping motion until a periodic flow behavior is reached. Once the unit gradient vector is evaluated, an optimization step, $\Delta\vec{S} = \varepsilon\frac{\vec{\nabla} O}{|\vec{\nabla} O|}$, is taken along the vector. This process continues until a local maximum in the optimization space is reached. The stepsize ε is evaluated by a line search along the gradient vector, at every optimization step.

Table 1: Optimization cases

Case	k	h_0	$P_{1\alpha}$	$P_{2\alpha}$	P_{0h}	P_{1h}	P_{2h}	$P_{0\alpha}$	α_0	ϕ
1	1.0	0.5	1.0	1.0	V	V	V	0.0	10^o	90^o
2	1.0	0.5	1.0	1.0	0.0	1.0	1.0	V	V	V

Table 2: RSM Design Points

Case **1**	P_{0h}	P_{1h}	P_{2h}
1	0.0	0.2	0.2
2	0.0	0.2	5.0
3	0.0	5.0	0.2
4	0.0	5.0	5.0
5	−0.9	1.0	0.2
6	−0.9	1.0	5.0
7	0.9	1.0	0.2
8	0.9	1.0	5.0
9	−0.9	0.2	1.0
10	−0.9	5.0	1.0
11	0.9	0.2	1.0
12	0.9	5.0	1.0
13	0.0	1.0	1.0

Case **2**	$\alpha_o(^o)$	$\phi(^o)$	$P_{0\alpha}$
1	5.0	30.0	0.0
2	5.0	150.0	0.0
3	35.0	30.0	0.0
4	35.0	150.0	0.0
5	5.0	90.0	−0.9
6	5.0	90.0	0.9
7	35.0	90.0	−0.9
8	35.0	90.0	0.9
9	20.0	30.0	−0.9
10	20.0	30.0	0.9
11	20.0	150.0	−0.9
12	20.0	150.0	0.9
13	20.0	90.0	0.0

Table 3: Initial conditions for steepest ascent method

Case	k	h_0	$P_{1\alpha}$	$P_{2\alpha}$	P_{0h}	P_{1h}	P_{2h}	$P_{0\alpha}$	α_0	ϕ	C_t
1	1.0	0.5	1.0	1.0	**0.0**	**1.0**	**1.0**	0.0	10^o	90^o	0.14
2	1.0	0.5	1.0	1.0	0.0	1.0	1.0	**0.0**	$\mathbf{20^o}$	$\mathbf{90^o}$	0.09

In the optimization studies, the flatness of the NURBS curve may be constrained through P_1 and P_2 parameters in order to exclude curves with large curvatures, which indicate the regions of large accelerations along the flapping path. Similarly, the center of rotation, P_o may also be constrained to prevent very large accelerations along a periodic motion.

Parallel Processing

In the solution of unsteady flows, a parallel algorithm based on domain decomposition is implemented in a master-worker paradigm. The C-grid is partitioned into overlapping subgrids first, and the solution on each subgrid is computed as a separate process in the computer cluster. The flow variables at the overlapping subgrid boundaries are exchanged among the subgrid processes at each time step of the unsteady solution. `PVM` (version 3.4.5) library routines are used for inter-process communication. In the optimization process, the components of the gradient vector which require unsteady flow solutions with perturbed optimization variables, are also computed in parallel. Computations are performed in a cluster of Linux based computers with dual Xeon and Pentium-D processors.

RESULTS

In this study, the maximization of thrust generation for a non-sinusoidally flapping airfoil is performed by first using RSM and then by a gradient based optimization method. The unsteady, laminar flow solutions over flapping airfoils are obtained by a Navier-Stokes solver in a parallel computing environment. The flowfields are computed at a low Mach number of 0.1 and a Reynolds number of 10000. The values for the reduced flapping frequency, $k \equiv \frac{\omega c}{U_\infty}$, and the plunge amplitude, h_0, are fixed at $k = 1.0$ and $h_0 = 0.5$.

Two optimization cases are studied as given in Table 1, where the optimization variables are denoted by V. In the first case, the flapping motion is a combination of non-sinusoidal plunging and sinusoidal pitching. For this case, the optimization variables are the NURBS parameters defining the plunging path, P_{0h}, P_{1h} and P_{2h} (Figure 3). Case 2 is a combination of non-sinusoidal pitching and sinusoidal plunging. The optimization variables for this case are the pitch amplitude, α_0, the phase shift between plunging and pitching, ϕ, and the NURBS parameter, $P_{0\alpha}$.

Table 4: Optimization results

Case 1	P_{oh}	P_{1h}	P_{2h}	C_t
RSM	0.9	5.0	5.0	**0.59**
Steepest Ascent	0.9	5.0	5.0	**0.58**

Case 2	$\alpha_o(^o)$	$\phi(^o)$	$P_{0\alpha}$	C_t
RSM	9.3	90.6	0.03	**0.17**
Steepest Ascent	9.2	90.7	-0.01	**0.15**

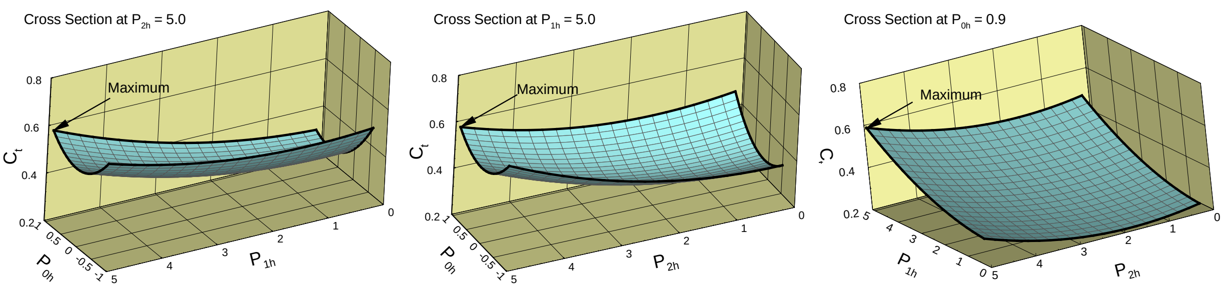

Figure 5: Response surfaces for Case 1

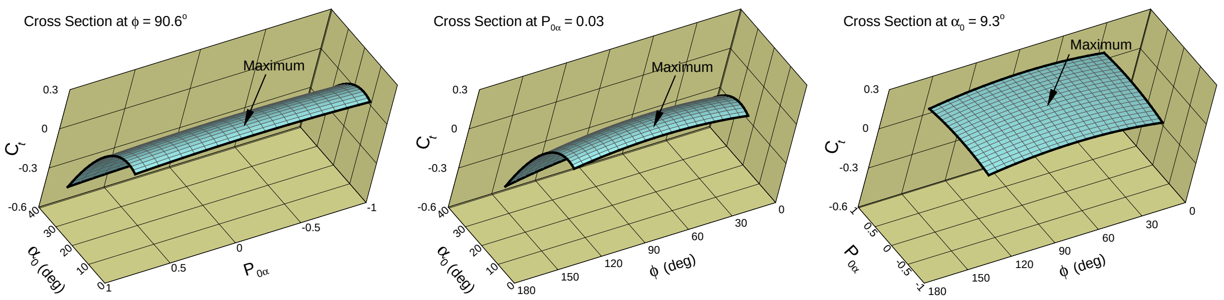

Figure 6: Response surfaces for Case 2

In this study, the P_1 and P_2 values are constrained within the range 0.2 to 5.0, and P_0 in the range -0.9 to 0.9, in order to define a proper flapping motion which does not impose excessively large accelerations. A flapping motion with very large instantaneous accelerations causes numerical difficulties in reaching periodic flow solutions, and is, in fact, not practical due to the inertial effects. It should be noted that the NURBS parameters, $P_0 = 0.0$, $P_1 = 1.0$, $P_2 = 1.0$, define a sinusoidal flapping motion.

Table 2 gives the design points used for constructing the response surfaces for Case 1 and 2. Design points are chosen based on Box-Behnken matrix of runs[27]. In each case, unsteady Navier-Stokes solutions are computed for 13 flapping parameter combinations given in the table. All the solutions are computed in parallel in a PC cluster. The computations for each case take about 2 hours of wall clock time using 40 processors. Once the design runs are completed, response surfaces are built by solving the least-square problem given in Equation 4. Least-square residuals of the RSM approximations are 0.005 and 0.001 for Case 1 and 2, respectively. The cross sections of the constructed response surfaces are shown in Figures 5 and 6 for Cases 1 and 2, respectively. As seen, the response surfaces are rather smooth. The optimum points where the thrust production is maximum are marked in the figures. It is noted that the optimum flapping motion for Case 1 at the constraint boundary.

The same optimization cases are also studied using the steepest ascent method. The initial conditions required for this method are given in Table 3. The NURBS parameters in the initial conditions define a sinusoidal flapping motion. For the optimization cases studied, parallel computations take about $15-30$ hours of wall clock time using 15 processors. The variation of NURBS parameters along the steepest ascent steps for Case 1 are shown in Figure 7. As all the optimization variables are incremented in the direction of the gradient vector, the average thrust coefficient increases gradually from $C_t = 0.14$, which is value for the sinusoidal flapping motion, and reaches a maximum value of $C_t = 0.58$. The corresponding propulsive efficiency is about 9% in contrast to the starting value of $\eta = 48\%$. Figure 8 shows the optimization steps for Case 2.

Table 4 gives the non-sinusoidal optimization results based on the RSM and the steepest ascent method. As seen from the table, the results are in a good agreement with each other. The performances of the RSM and the steepest ascent method are given in Figures 9 and 10 in terms of the number of the functions evaluations. Each function evaluation is an unsteady flow solution over a flapping airfoil for the given flapping parameters. In both cases RSM

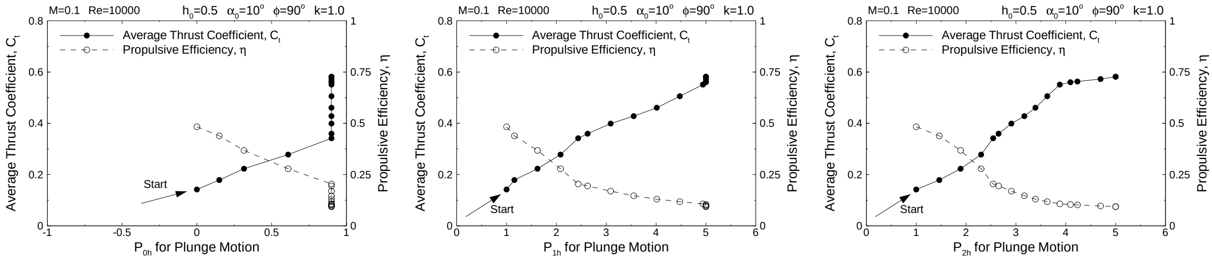

Figure 7: Steepest ascent steps for Case 1

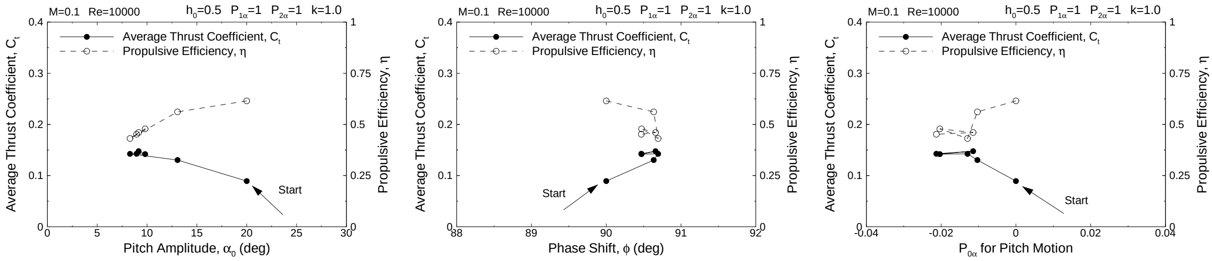

Figure 8: Steepest ascent steps for Case 2

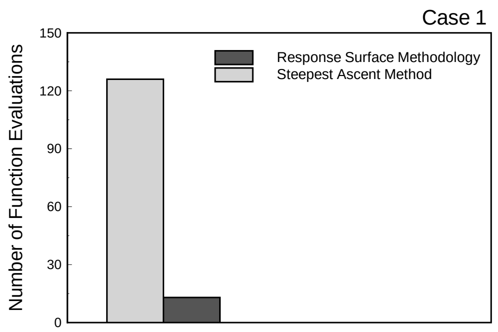

Figure 9: Number of function evaluations for Case 1

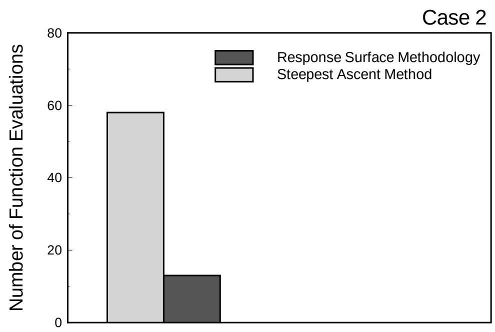

Figure 10: Number of function evaluations for Case 2

uses 13 function evaluations since there are 3 variables in each case[27]. In Case 1, the steepest ascent method requires 126 functions evaluations for convergence while the second case requires 58 functions evaluations. In RSM The number of function evaluations is significantly smaller in RSM than in the steepest ascend method, while the optimum solution is about the same in both cases.

CONCLUSIONS

In this study, the thrust generation of a non-sinusoidally flapping airfoil is approximated using RSM. The non-sinusoidal flapping motion is defined by NURBS. The NURBS parameters are successfully used to construct the response surfaces. The response surface approximations are generated using various Navier-Stokes solutions of the laminar flows over a flapping airfoil. The maxima of the response surfaces give the optimum flapping motions which provide maximum thrust. The same optimization cases are also studied using the steepest ascent method. The results show that both methods are in a well agreement with each other. It is observed that RSM uses significantly less number of function evaluations than steepest ascent uses. For the cases studied, an optimization based on RSM takes less time for convergence when compared to the steepest ascent method. Further research is in progress to include all the NURBS parameters as optimization variables.

References

[1] Kaya, M. and Tuncer, I.H., *Non-Sinusoidal Path Optimization of Flapping Airfoils*, AIAA Journal, Vol. 45, No. 8, 2007, pp. 2075-2082.

[2] Lee, J.-S., Kim, C. and Kim, K. H., *Design of Flapping Airfoil for Optimal Aerodynamic Performance in Low-Reynolds Number Flows*, AIAA Journal, Vol. 44, No. 9, 2006, pp. 1960-1972.

[3] Heatcote, S., Wang, Z. and Gursul, I., *Effect of Spanwise Flexibility on Flapping Wing Propulsion*, 36th Fluid Dynamics Conference and Exhibit, AIAA, San Francisco, CA, No. 2006-2870, June 2006.

[4] Tuncer, I.H. and Kaya, M., *Optimization of Flapping Airfoils For Maximum Thrust and Propulsive Efficiency*, AIAA Journal, Vol. 43, No. 11, 2005, pp. 2329-2341.

[5] Kaya, M. and Tuncer, I.H., *Path Optimization of Flapping Airfoils for Maximum Thrust Based on Unsteady Viscous Flow Solutions*, 3rd Ankara International Aerospace Conference, Middle East Technical University, Ankara, Turkey, Aug. 2005.

[6] Schouveiler, L., Hover, F. S. and Triantafyllou, M. S., *Performance of Flapping Foil Propulsion*, Journal of Fluids and Structures, Vol. 20, No. 7, Special Issue, 2005, pp. 949-959.

[7] Hover, F. S., Haugsdal, Ø. and Triantafyllou, M. S., *Effect of Angle of Attack Profiles in Flapping Foil Propulsion*, Journal of Fluids and Structures, Vol. 19, No. 1, 2004, pp. 37-47.

[8] Young, J. and Lai, J.C.S., *Oscillation Frequency and Amplitude Effects on the Wake of a Plunging Airfoil*, AIAA Journal, Vol. 42, No. 10, 2004, pp. 2042-2052.

[9] Jones, K.D. and Platzer, M.F., *Experimental Investigation of the Aerodynamic Characteristics of Flapping-Wing Micro Air Vehicles*, 41st Aerospace Sciences Meeting and Exhibit, AIAA, Reno, NV, No. 2003-418, Jan. 2003.

[10] Jones, K.D., Castro, B.M., Mahmoud, O., Pollard, S.J., Platzer, M.F., Neef, M.F., Gonet, K., Hummel, D. *A Collaborative Numerical and Experimental Investigation of Flapping-Wing Propulsion*, 40th Aerospace Sciences Meeting and Exhibit, AIAA, Reno, NV, No. 2002-706, Jan. 2002.

[11] Jones, K.D., Duggan, S.J., Platzer, M.F., *Flapping-Wing Propulsion for a Micro Air Vehicle*, 39th Aerospace Sciences Meeting and Exhibit, AIAA, Reno, NV, No. 2001-126, Jan. 2001.

[12] Mueller, T.J. (ed.), *Fixed and Flapping Wing Aerodynamics for Micro Air Vehicles*, Progress in Aeronautics and Astronautics, AIAA, Reston, VA, 2001, Vol. 195.

[13] Tuncer, I.H. and Platzer, M.F., *Computational Study of Flapping Airfoil Aerodynamics*, AIAA Journal of Aircraft, Vol. 37, No.3, 2000, pp. 514-520.

[14] Platzer, M.F. and Jones, K.D., *The Unsteady Aerodynamics of Flapping-Foil Propellers*, 9th International Symposium on Unsteady Aerodynamics, Aeroacoustics and Aeroelasticity of Turbomachines, Ecole Centrale de Lyon, Lyon, France, Sept. 2000.

[15] Isogai, K., Shinmoto Y., Watanabe, Y., *Effects of Dynamic Stall on Propulsive Efficiency and Thrust of a Flapping Airfoil*, AIAA Journal, Vol. 37, No. 10, 1999, pp. 1145-1151.

[16] Shyy, W., Berg, M. and Lyungvist, D., *Flapping and Flexible Wings for Biological and Micro Air Vehicles*, Progress in Aerospace Sciences, Elsevier, Exeter, UK, 1999, Vol. 35, No.5, pp. 455-505.

[17] Lai, J.C.S. and Platzer, M.F., *Jet Characteristics of a Plunging Airfoil*, AIAA Journal, Vol. 37, No. 12, 1999, pp. 1529-1537.

[18] Jones, K.D., Dohring, C.M. and Platzer, M.F., *Experimental and Computational Investigation of the Knoller-Beltz Effect*, AIAA Journal, Vol. 36, No. 7, 1998, pp. 1240-1246.

[19] Anderson, J.M., Streitlen, K., Barrett, D.S. and Triantafyllou, M.S., *Oscillating Foils of High Propulsive Efficiency*, Journal of Fluid Mechanics, Vol. 360, Apr. 1998, pp. 41-72.

[20] Piegl, L. and Tiller, W., *The NURBS Book*, 2^{nd} ed., Springer-Verlag, Berlin, 1997, Chap. 4.

[21] Tuncer, I.H., Lai, J., Ortiz, M.A. and Platzer, M.F., *Unsteady Aerodynamics of Stationary/Flapping Airfoil Combination in Tandem*, 35th Aerospace Sciences Meeting and Exhibit, AIAA, Reno, NV, No. 1997-659, Jan. 1997.

[22] Tuncer, I.H. and Platzer, M.F., *Thrust Generation due to Airfoil Flapping*, AIAA Journal, Vol. 34, No. 2, 1996, pp. 324-331.

[23] Roux, W.J., Stander, N. and Haftka, R.T., *Response Surface Approximations for Structural Optimization*, International Journal for Numerical Methods in Engineering, Vol. 42, 1998, pp. 517-534.

[24] S. N. Gangadharan, R. T. Haftka and Y. I. Fiocca, *Variable-complexity-modelling structural optimization using response surface methodology*, AIAA paper 95-1164, Presented at the 36th AIAA/ASME/ASCE/AHS/ASC Structures, Structural Dynamics and Materials Conference, 10-12 April, New Orleans, LA, 1995.

[25] A. A. Giunta, J. M. Dudley, R. Narducci, B. Grossman, R. T. Haftka, W. H. Mason and L. T. Watson, *Noisy aerodynamic response and smooth approximations in HSCT Design*, AIAA Paper 94-4376-CP, Presented at the AIAA/NASA/USAF/ISSMO Symp. on Multidisciplinary Analysis and Optimization, Panama City, FL, 1994.

[26] D. H. Van Campen, R. Nagtegaal and A. J. G. Schoofs, *Approximation methods in structural optimization using experimental designs for for multiple responses*, in H. Eschenauer, J. Koski and A. Osyczka (eds.), Multicriteria Design Optimization, Springer, Berlin, 1990, pp. 205-228.

[27] Box, G. E. P. and Behnken, D. W., *Some new three level designs for the study of quantitative variables*, Technometrics, Vol. 2, pp. 455475.